

In conclusion, optimized geometries, charge distributions, and molecular orbital structure were generated for MPTP and intermediates in its conversion to MPP⁺. Sequential electron, proton, electron mechanisms as well as electron, hydrogen atom and concerted hydride transfer were considered. The data show the initial ionization of MPTP is highly energetic and results in the

formation of intermediates capable of interacting with O₂ to generate O₂^{•-} and possibly causing enzymatic inactivation or neurotoxicity. The large resonance energy of MPP⁺ was demonstrated as well as the potent reducing potential of MPP⁺. In addition, the reaction of MPTP was shown to be both quantitatively and qualitatively different from the oxidation of an NADH analogue.

(27) (a) Ohno, A.; Shio, T.; Yamamoto, H.; Oka, S. *J. Am. Chem. Soc.* **1981**, *103*, 2045-2048. (b) Carlson, B. W.; Miller, L. L.; Neta, P.; Grodkowski, J. *J. Am. Chem. Soc.* **1984**, *106*, 7233-7239. (c) Powell, M. F.; Wu, J. C.; Bruice, T. C. *J. Am. Chem. Soc.* **1984**, *106*, 3850-3856.

Acknowledgment. The authors would like to thank Ms. Anna Marie Martin for her help in preparing this manuscript. This work was supported in part by a grant from the NIH (GM 27167).

Resonance Raman Studies of Myoglobin Single Crystals

Dimitrios Morikis, J. Timothy Sage, Apostolos K. Rizos,[†] and Paul M. Champion*

Contribution from the Department of Physics, Northeastern University, Boston, Massachusetts 02115. Received November 2, 1987

Abstract: We investigate the resonance Raman scattering of myoglobin (Mb) single crystals in order to probe the similarities and/or differences between solution and crystal structures of biological molecules. Resonant light scattering spectroscopy provides a high-resolution map of the vibrational frequencies associated with the protein active site and can be applied to solution, crystalline, or frozen states of the sample. We find that the metmyoglobin samples have active site heme structures that are nearly independent of the sample state. However, when the carbon monoxide adduct is formed, the MbCO crystal spectrum reveals two distinct modes of CO binding, compared to a single Raman mode in the solution structure. Unusual observations involving the photoreduction of metMb and the photolysis of MbCO in the crystalline state are also reported. A preliminary polarization analysis of the Raman scattering from Mb crystals is also presented.

We present resonance Raman spectra of single crystals of myoglobin (Mb) and compare them to solution spectra. With some key exceptions, the relative Raman intensities and frequencies of the crystals are found to be nearly identical with the solution samples. The polarization of the Raman scattering is also analyzed and the depolarization ratios ($\rho = I_{\perp}/I_{\parallel}$) of the heme vibrations in metMb are found to vary strongly with the crystal orientation. An increase of the laser flux at the metMb crystal leads to a photoreduction process that produces a species whose Raman spectrum is nearly identical with that of deoxymyoglobin. Carbon monoxide bound myoglobin crystals (MbCO) are also examined. We find two different types of CO binding in the room temperature crystal as evidenced by their distinct Fe-CO vibrational frequencies at 491 and 508 cm⁻¹. Surprisingly, we are unable to completely photodissociate the MbCO crystals in order to examine the deoxy photoproduct. This suggests that the CO is trapped in the distal pocket of the MbCO crystal at room temperature and that the geminate rebinding rates are rapid compared to the laser-driven photolysis.

The Raman spectra are collected with use of continuous wave laser excitation wavelengths in the region $\lambda_{\text{ex}} = 415-430$ nm, which is resonant with the Soret band of heme proteins. The detection of the scattered radiation is accomplished with use of an intensified diode array detector and a triple grating spectrograph. The crystals are grown according to the method of Kendrew and Parrish¹ with use of sperm whale metMb obtained commercially. The crystallographic coordinates of Takano are used to obtain the heme orientations.²

Figure 1 displays the high-frequency (950-1700 cm⁻¹) and the low-frequency (200-950 cm⁻¹) Raman spectra of metMb under three different conditions (crystal high-flux, crystal low-flux, and solution). The high laser flux condition (ca. 30 W/cm²) leads

to an apparent photoreduction of the metMb crystal (a). This is evidenced by the shift of the oxidation state marker band³ (ν_4) from 1372 to 1355 cm⁻¹ as well as by the appearance of the iron-histidine axial ligand mode ($\nu_{\text{Fe-His}}$) at 219 cm⁻¹.

Upon detailed comparison of the crystal and solution Raman spectra (b and c), we find no reproducible frequency differences between the two species. This provides the first direct, high-resolution, spectroscopic evidence that the active site heme structure is unperturbed upon crystallization. The favorable comparison between crystal and solution structures is reminiscent of early cryogenic resonance Raman studies of heme proteins⁴ where it was shown that the heme structure was not detectably modified upon freezing the solution. It seems that the interaction of the globular protein material and the heme group is remarkably stable to perturbations induced by phase change.

In Figure 2 we display resonance Raman spectra of MbCO crystals, formed using the method described by Kuriyan et al.⁵ The Fe-CO stretching mode found⁶ near 500 cm⁻¹ is of particular interest, since the presence of two vibrational frequencies at 508 and 491 cm⁻¹ is clearly visible in the crystal data (trace b). The solution spectra are dominated by the presence of a single mode at 508 cm⁻¹ (trace c). This implies that the relative populations of distal pocket structures, responsible for the orientation and/or polarization of the Fe-CO moiety, are different in crystalline material than in solution at pH 7. The observation of multiple

(1) Kendrew, J. C.; Parrish, R. G. *Proc. R. Soc. London A* **1956**, *238*, 305-324.

(2) Takano, T. *J. Mol. Biol.* **1977**, *110*, 537-568.

(3) Spiro, T. G. In *Iron Porphyrins*, Part II; Lever, A., Gray, H., Eds.; Addison-Wesley: Reading, MA, 1983.

(4) Champion, P. M.; Collins, D. W.; Fitchen, D. B. *J. Am. Chem. Soc.* **1976**, *98*, 7114-7115.

(5) Kuriyan, J.; Wilz, S.; Karplus, M.; Petsko, G. *J. Mol. Biol.* **1986**, *192*, 133-154.

(6) Tsubaki, M.; Srivastava, R.; Yu, N. T. *Biochemistry* **1982**, *21*, 1132-1140.

[†] Present address: Department of Chemistry, University of Crete, 711 10 Iraklion, Greece.

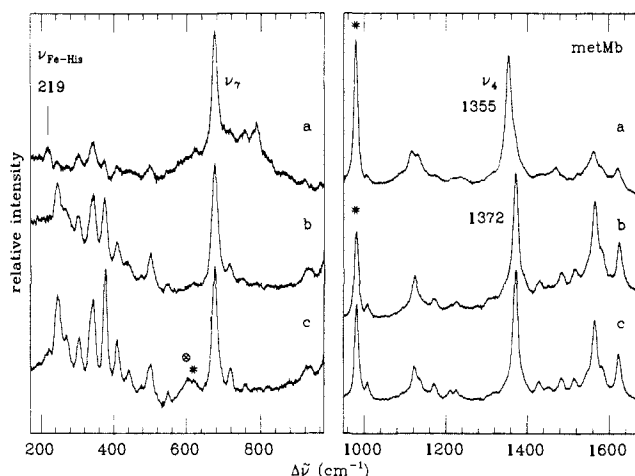


Figure 1. Resonance Raman spectra of the high-frequency region of photoreduced Mb crystal (a), metMb crystal (b), and metMb solution (c). The spectra of the high-frequency modes are normalized to the peak height of the strongest protein peak, ν_4 . The low-frequency spectra are normalized to ν_7 . The peaks marked with an asterisk are due to sulfate and \odot denotes laser emission. The excitation wavelength is 430 nm for spectrum a and 415 nm for spectra b and c. The slit resolution is 7.5 cm^{-1} in all spectra.

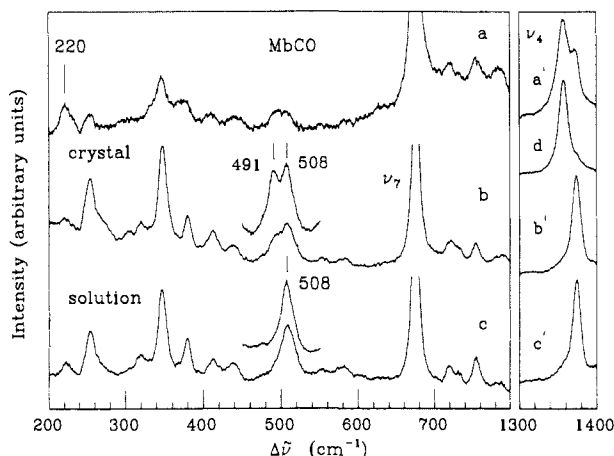


Figure 2. Resonance Raman spectra of MbCO solution and crystal recorded at low frequencies (traces a-c) and in the region of the oxidation marker band (traces a'-c'). Traces a and a' were taken on a MbCO crystal at high laser intensity (29 mW, focused beam). The appearance of the 220- and 1355- cm^{-1} Raman modes indicates the presence of deoxyMb. The CO-bound material is indicated by the modes at 1375 and ca. 500 cm^{-1} . Traces b and b' show the MbCO crystal spectrum taken with low laser intensity (5.5 and 14 mW, respectively, defocused beam). The insert shows the two Fe-CO vibrational modes at high resolution. Traces c and c' show the MbCO solution spectrum taken with low laser intensity (5.5 mW, defocused beam) using a spinning cell. For a stationary MbCO solution at high laser intensity (16 mW, focused beam), complete CO dissociation is indicated by the existence of a single peak at 1355 cm^{-1} (trace d). The excitation wavelength of all spectra (except the inserts) is 430 nm and the slit resolution is 7.5 cm^{-1} . The inserts in traces b and c are taken with $\lambda_{\text{ex}} = 420$ nm and a slit of 4.5 cm^{-1} (trace b) and 2.3 cm^{-1} (trace c) using a scanning double monochromator.

Fe-CO species in crystals is in agreement with the X-ray structure analysis⁵ as well as early infrared studies.⁷ Raman spectra have also detected multiple Fe-CO frequencies in solutions of MbCO.

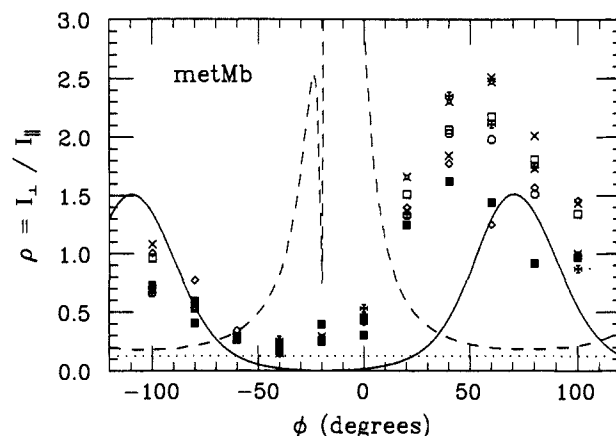


Figure 3. Plot of depolarization ratio as a function of orientation angle of several A_{1g} modes of the metMb crystal. The variable ϕ represents the experimental goniometer setting used when rotating the crystal in the laboratory frame. \times , 1565 cm^{-1} ; \diamond , 1483 cm^{-1} ; \square , 1372 cm^{-1} ; \circ , 677 cm^{-1} ; \times , 375 cm^{-1} ; \boxtimes , 344 cm^{-1} . The solid curve is generated with a theoretical simulation assuming only in-plane polarizability for the two heme sites. The dotted line at the bottom shows the theoretical value of ρ for A_{1g} modes in solution ($\rho = 1/8$). The solid squares show the 246- cm^{-1} mode assigned to the Fe-N_{His} vibration. The predicted depolarization ratio for a z-polarized charge-transfer resonance is shown as the dashed line (the rapid change in ρ near $\phi = -20^\circ$ in the z-polarized simulation occurs when the heme planes, occupying one of the two sites, become parallel to the incident polarization direction).

where pH and temperature have been shown to regulate the relative concentrations of the two major species.⁸

The right side of Figure 2 shows the oxidation marker band region of MbCO. When the laser power is increased, the formation of some deoxyMb is observed (trace a'); however, the crystal cannot be completely driven to deoxyMb, using laser powers below the crystal burning threshold. This indicates that significant diffusion of the CO out of the heme pocket does not take place in the crystal sample. The geminate rebinding process can thus be probed at room temperature for first time, independently from the diffusion processes that influence the kinetics in liquid phase.

In Figure 3 we present the results of depolarization ratio measurements on metMb. In solution, the random orientation of the molecules results in averaging the polarizability tensor so that $\rho = 1/8$ for A_{1g} modes in D_{4h} symmetry (dotted line). The values of ρ can be predicted in the crystalline sample when the heme orientations are known with respect to the crystal axes.² The solid curve in Figure 3 is generated under the assumptions of D_{4h} symmetry and vanishing out-of-plane polarizability for each of the two heme sites in the unit cell. The fact that the theoretical curve and the data follow the same general trend is encouraging. A much more detailed polarization analysis that includes the effects of lower symmetry and/or out-of-plane polarizability will be presented elsewhere.⁹

Acknowledgment. This work is supported by the National Institutes of Health (DK 35090) and the National Science Foundation (DMB 84-17712). P.M.C. is the recipient of a NIH career development award (DK 01405).

Registry No. Heme, 14875-96-8.

(8) Reinisch, L.; Srajer, V.; Champion, P. M. *Bull. Am. Phys. Soc.* **1987**, *33*, 1412.

(9) Sage, J. T.; Morikis, D.; Champion, P. M. *J. Chem. Phys.*, submitted for publication.

(7) Makinen, M.; Houtchens, R.; Caughey, W. *Proc. Natl. Acad. Sci.* **1979**, *76*, 6042-6046.